ФИЗИКА ЭЛЕМЕНТАРНЫХ ЧАСТИЦ И АТОМНОГО ЯДРА
2016. Т. 47. ВЫП. 6

LATEST RESULTS FROM DOUBLE CHOOZ

A. Minotti on behalf of Double Chooz Collaboration*

Université de Strasbourg, IPHC, Strasbourg, France

Double Chooz is a short-baseline neutrino disappearance experiment. It detects $\bar{\nu}_e$ produced in the power plant of Chooz, France, where is located. The main goal of the experiment is the measurement of θ_{13} mixing angle and in 2011 for the first time the experiment observed an indication for a non-zero value of such an oscillation parameter. The mixing angle was successively measured using only the far detector finding the best fit value of $\sin^2(2\theta_{13}) = 0.090^{+0.032}_{-0.029}$. The near detector is under construction and will start data taking by the middle of 2014, allowing the reduction of the systematic errors. In this paper I make a review of the Double Chooz experiment, focusing in particular on the latest results of the measurement of the mixing angle θ_{13} relying on the neutron absorption on gadolinium. I also present results proving the capability of Double Chooz to identify the ortho-positronium. This has been done on an event-by-event basis for the first time in a large liquid scintillator experiment and can be an additional handle for the electron/positron discrimination in future detectors based on such a technology.

PACS: 23.40.-s; 23.40.Bw

INTRODUCTION

The standard three-families neutrino oscillation can be described by three mixing angles, two independent mass square differences, and a CP-violation phase. Among the three mixing angles, θ_{13} is the smallest and was the last to be measured. Double Chooz was the first experiment to show a hint of a non-zero value of θ_{13} [1] and currently plays an important role in the race to improve the precision on this parameter, along with two other reactor neutrino experiments, Daya Bay [2] and RENO [3], and the accelerator neutrino experiment T2K [4]. This discovery of a non-zero θ_{13} paved the way for designing of future experiment aiming to measure the CP-violation in the leptonic sector.

Double Chooz detects reactor $\bar{\nu}_e$ via inverse beta decay (IBD), with the signature given by a delayed coincidence between the positron signal and the neutron capture. Basing on which nucleus captures the neutron, we distinguish between

*E-mail: alessandro.minotti@iphc.cnrs.fr

hydrogen (n-H) and gadolinium (n-Gd) analysis, with the former being exploited by Double Chooz for the first time [5]. The n-Gd analysis has seen a major improvement in the last publication [6], with respect to the previous results of [7].

This article is focused on these latest results.

1. EXPERIMENTAL CONCEPT

As a reactor neutrino oscillation experiment, Double Chooz aims to measure θ_{13} by looking at the disappearance of $\bar{\nu}_e$ produced in nuclear fissions happening inside a power reactor. The survival probability of $\bar{\nu}_e$ can be expressed by

$$P(\bar{\nu}_e \to \bar{\nu}_e) \simeq 1 - \sin^2(2\theta_{13}) \sin^2\left(\frac{\Delta m^2_{23} L}{4E}\right) - \cos^4(\theta_{13}) \sin^2(2\theta_{12}) \sin^2\left(\frac{\Delta m^2_{12} L}{4E}\right), \quad (1)$$

where $L\,(\mathrm{km})$ is the distance between the neutrino source and the detector, or baseline, $E\,(\mathrm{MeV})$ the neutrino energy, Δm^2_{23} and Δm^2_{12} the atmospheric and solar mass splitting, θ_{12} and θ_{13} two of the three mixing angles. The nature of the two mass splitting is so that the two terms (the two lines of Eq. 1) govern the oscillation at different baselines, with the first term (atmospheric oscillation) dominating at $L/E < 10$ km/MeV. In Double Chooz, a near detector placed at a short baseline of about 400 m (i.e., where the oscillation probability is basically zero) and a far detector at a baseline of 1050 m (corresponding to about the maximal atmospheric oscillation probability and no solar oscillation) measure $\bar{\nu}_e$ rate and spectrum before and after the oscillation occurs. A distortion between neutrino spectra measured by the near and the far detector is a signature of a non-zero value of the atmospheric oscillation amplitude $\sin^2(2\theta_{13})$.

The Double Chooz far detector has been operating since April 2011, with a Monte Carlo simulation of the expected non-oscillated $\bar{\nu}_e$ spectrum working as an effective near detector. As a consequence, the systematic error on θ_{13} measure mainly comes from the reactor flux uncertainty. This limits the current precision of the one-detector data analysis, which reaches a relative error of 30% on $\sin^2(2\theta_{13})$. The actual near detector had its commissioning started in January 2015, and is currently collecting data. A cancellation of several systematics contributions is foreseen for the forthcoming two-detectors analysis, with the possibility to achieve a final precision of about 10% on $\sin^2(2\theta_{13})$.

2. NEUTRINO DETECTION

Neutrinos are detected via the Inverse Beta Decay (IBD) process

$$\bar{\nu}_e + p \to e^+ + n, \quad (2)$$

which has an energy threshold of 1.8 MeV. The neutrino energy spectrum is a convolution of the reactor flux and the IBD cross section, resulting in an energy range of 2 to 8 MeV peaked at ~ 4 MeV. Since the oscillation probability depends on the neutrino energy, a measure of E_ν allows a shape oscillation analysis (see Sec. 7). E_ν is directly related to the energy of the positron

$$E_{e^+} \simeq E_\nu - 0.8 \text{ MeV}, \tag{3}$$

which can be measured inside the liquid scintillator.

The signature of an IBD interaction is given by a two-fold coincidence (time and space correlation) between the positron ionization and annihilation (prompt signal), and the γ's emitted in the neutron capture (delayed signal). The delayed neutron capture can be either on Gd, with a total released energy of ~ 8 MeV and a mean delayed Δt of ~ 30 μs with respect to the prompt signal, or on hydrogen, in which case the released energy is 2.2 MeV and the mean $\Delta t \sim 200$ μs.

3. DETECTOR LAYOUT

Each Double Chooz detector (Fig. 1) consists of four concentric cylinders, an outer veto (OV), and calibration devices. The innermost cylinder is the 10.3 m^3 neutrino target, consisting in an acrylic vessel filled with a PXE-based liquid scintillator (LS) doped with gadolinium (Gd) at 1 g/l. The Gd increases the detection efficiency by providing a large n capture cross section and released

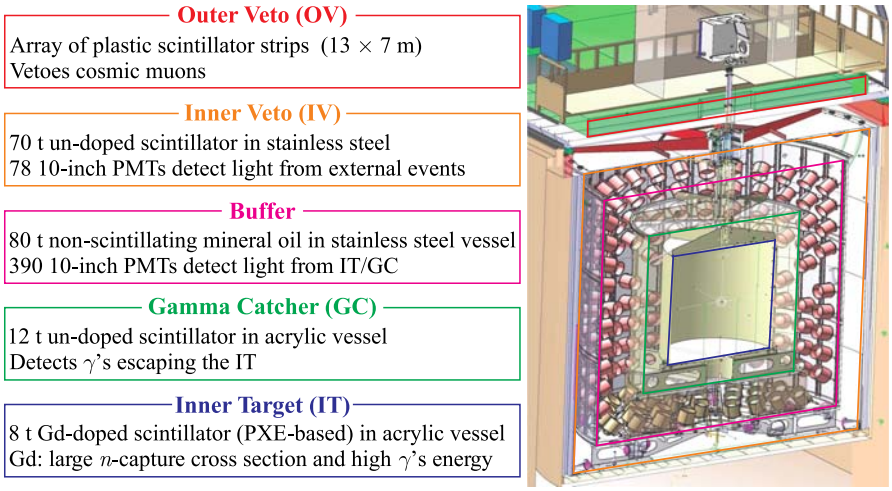

Fig. 1. Double Chooz detector design

energy. The target is surrounded by a 22.5 m^3 gamma catcher, in an acrylic vessel, filled with a similar un-doped LS, which collects γ's escaping the target. In turn the gamma catcher is surrounded by the buffer, a 105 cm thick layer of non-scintillating mineral oil placed in a stainless steel tank. Light from the target and the gamma catcher is collected by 390 10-inch PMTs installed on the inner wall of the buffer tank. Outside the buffer, and optically isolated from it, is the inner veto (IV), a 50 cm thick layer of LS in a steel tank equipped with 78 8-inch PMTs serving as a veto from external events.

Above the detector is the outer veto (OV), a scintillator-strip-based muon tracking system. The chimney connects the inner volumes with the exterior, and it is used to introduce calibration sources in the detector. Deployed (^{137}Cs, ^{68}Ge, ^{60}Co and ^{252}Cf) and natural (neutrons, Bi–Po coincidences) sources are used in combination with a multi-wavelength LED-fibre light injection system to calibrate the detector.

4. NEUTRINO RATE PREDICTION

$\bar{\nu}_e$ are produced in the Chooz nuclear plant, which is operated by EDF*, as a result of β decays of fission products (^{235}U, ^{239}Pu, ^{238}U, ^{241}Pu). Each of the two reactor cores has a $4.25\,\mathrm{GW_{th}}$ maximal thermal power, for a combined flux of $\sim 10^{21}$ s^{-1}.

The neutrino rate expected in case of no oscillation is computed summing the contribution of the two reactors (R) as

$$N_\nu^{\exp}(E,t) = \sum_{R=1,2} \frac{N_p \epsilon}{4\pi L_R^2} \frac{P_R^{\mathrm{th}}(t)}{\langle E_f \rangle_R(t)} \sigma_f(E,t)\,. \tag{4}$$

The first term of Eq. (4) accounts for the number of protons of the target N_p, the detection efficiency (number of IBDs passing the selection) ϵ, and the solid angle, which depends on the baseline L. The second term represents the average number of fissions and is given by the reactor thermal power P^{th} divided by the average energy released per fission $\langle E_f \rangle$. P^{th} is provided by EDF, while $\langle E_f \rangle$ depends on the fuel composition, whose time evolution is simulated. Finally, the third term is the average cross section per fission, and it is based on the neutrino spectrum. The $\bar{\nu}_e$ rate is anchored to the value measured by Bugey4 [8], with corrections for the different fuel composition, to reduce the normalization uncertainty. The total systematic contribution associated with the flux prediction is 1.7%.

*Électricité de France.

5. NEUTRINO SELECTION

In Double Chooz, IBD from neutrino interactions are selected in two steps: first single energy depositions inside the target are recorded, then a delayed coincidence between two singles is required. For the measurement of the θ_{13} mixing angle, two different analyses were carried out using Gd and H as target nuclei for neutron absorption (delayed signal). While the gadolinium analysis has the advantage of a high-energy delayed signal, which results in a strong background suppression, the hydrogen one has the advantage of a larger statistics (by about a factor of 3 with respect to the Gd one).

For the singles, cosmic muons entering the detector are identified based on released energy criteria and rejected, as well as following events within a time window (1 ms veto). Light noise arising from spontaneous photoemission of some PMT bases is also rejected, based on the geometrical distribution of the touched PMT in the event as well as on their trigger time (more details can be found in [7]).

Table 1. **Neutrino candidates selection [6]**

Cut	Window
Prompt energy, MeV	$0.5-20$
Delayed energy, MeV	$4-10$
Time correlation, μs	$0.5-150$
Distance correlation, m	< 1
Isolation window (prompt), μs	–200–600

For IBD candidates, the selection depends on the analysis (Gd or H) and includes an isolation window around the prompt signal, a prompt and a delayed energy window, a correlation time and a correlation distance window. A summary of the neutrino selection used in [6] can be found in Table 1. Further cuts developed to veto the remaining background are shown in the next section.

6. BACKGROUND

There are three categories of background that can mimic the prompt-delay coincidence of an IBD: accidental coincidences, cosmogenic β–n emitters, and correlated background. The fraction of each background that survives the vetoes, along with the energy shape, is estimated and used as information in the final fit that determines θ_{13}. The estimated rates are resumed in Table 2.

The accidental background arises from an event in the prompt energy window that is incidentally in coincidence with a fast spallation neutron that gets absorbed

Table 2. **Estimated rates of main backgrounds**

Background	Rate
^{9}Li/^{8}He	$0.97^{+0.41}_{-0.16}$
Correlated	0.604 ± 0.051
Accidental	0.070 ± 0.003

on Gd (or H) within the allowed time window from the prompt signal. The prompt event is typically radioactivity originated in the surrounding rock or the PMTs. Spallation neutrons result from energetic cosmic muons hitting nucleons in the rock and thermalizing their way to the target before being captured. The accidental component left in neutrino candidates is estimated with off-time coincidences.

Cosmogenic background consists in long-lived β-n decaying isotopes, such as ^{9}Li or ^{8}He. They are produced by cosmic muons in the detector and can survive the muon isolation window (see Table 1) given their long lifetime, which is of the order of hundreds of milliseconds*. Cosmogenic events are identified and rejected with a likelihood based on the characteristics of events collected in an after-μ window. Tagged events are also used to evaluate the energy shape of the remaining background, while its rate is estimated looking at the correlation of events with the last muon.

Correlated background includes other processes that produce a prompt-delayed coincidence. Fast spallation neutrons can undergo nuclear interactions in the detector and produce recoil protons that ionize the scintillator (prompt signal), before being thermalized and captured (delayed signal). Stopping muons could enter the detector from the chimney and stop there, giving a small signal that could fake a prompt positron one. The Michel electron coming from the muon decays has a large energy spectrum that includes also the energy window selected for the neutron capture and can therefore fake a delayed signal. Correlated background is vetoed by excluding events for which the prompt signal is in coincidence with a trigger from the OV. The IV can tag fast neutrons, and it is used to veto and to estimate the rate and shape of the remaining background. Stopping muons are usually not tagged by the IV, which is blind to events that are inside the chimney, but are rejected by a cut on the goodness of the delayed vertex reconstruction.

7. θ_{13} ANALYSIS

We now discuss the sample, results and errors of the θ_{13} analyses of the latest n-Gd publication [6]. With respect to the previous n-Gd publication [7], we profit of an extended lifetime of 460.67 days. Thanks to an improved background

*257 ms for ^{9}Li, 171 ms for ^{8}He.

reduction, it was possible to widen the IBD selection and still have positive effect on the signal-on-background ratio. As a result, the statistics of [6] is doubled with respect to [7], for a total of 17351 IBD candidates. The uncertainties are also reduced of roughly 20%. The number of selected IBD candidates per day follows with a very good agreement with the reactor power, as shown in Fig. 2. In the figure, the two configurations with only one reactor on and two reactors on are highlighted, as well as two small periods of time in which both reactors were off (off-off period).

The off-off period is a unique feature of Double Chooz. It consists of 7.24 days in total, and the number of candidate IBDs is 7 events [9]. This number is compatible with the background model that predicts $12.9^{+3.1}_{-1.4}$ events.

Detection systematics are also evaluated, with reactor flux estimation carrying the larger errors, as already mentioned. Other systematics include the detection efficiency and the errors on the different backgrounds estimation. These values, along with the statistical error, are resumed in Table 3.

The expected number of events in absence of oscillations (i.e., assuming $\theta_{13} = 0$), the number of observed IBDs, and the contributions of each background

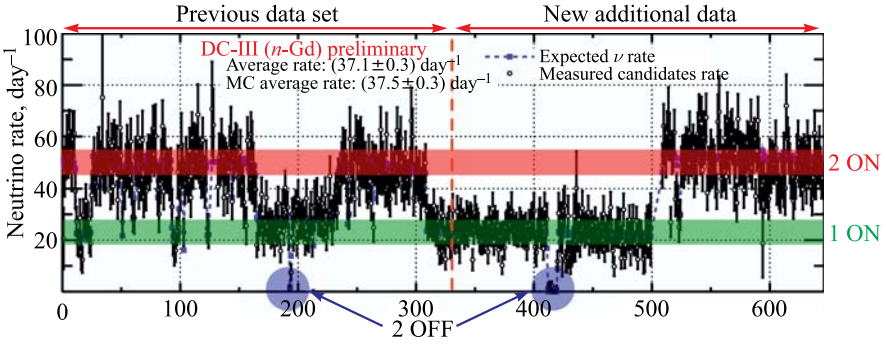

Fig. 2. Selected number of neutrino candidates day by day

Table 3. **Systematic uncertainties, as evaluated in [6]**

Uncertainty	Value, %
Reactor flux	1.7
Detection	0.6
Cosmogenic background	$+1.1/-0.4$
Correlated background	0.1
Statistics	0.8
Total	$+2.3/-2.0$

component (Table 2) are compared to estimate the value of θ_{13}. Two different fits have been developed to measure θ_{13}. In the *Rate + Shape* analysis, the energy

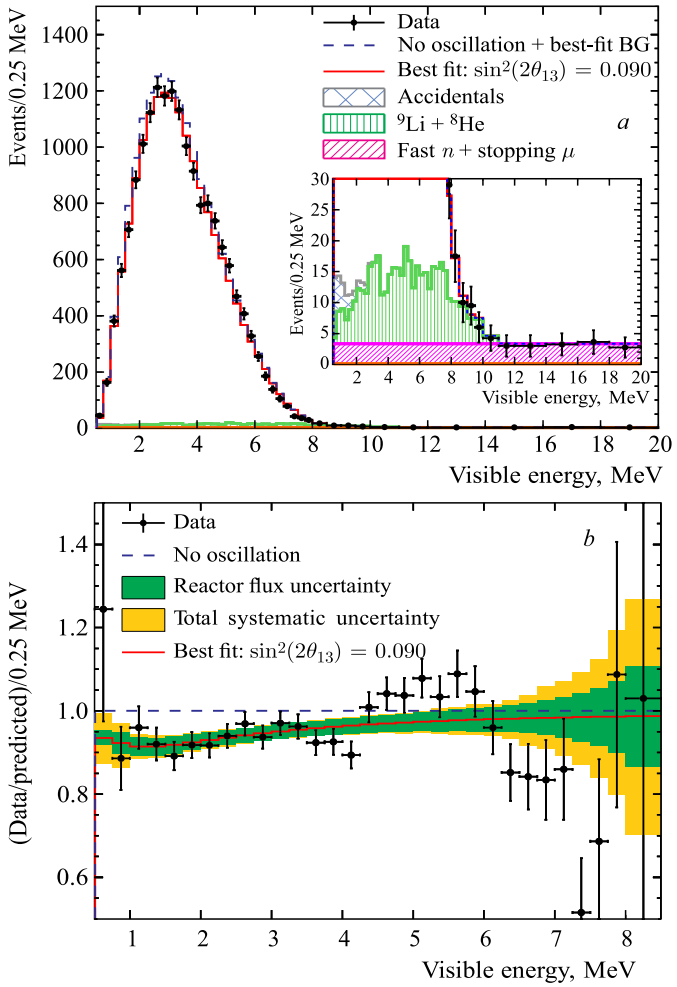

Fig. 3 (color online). *a*) Measured energy spectrum of the prompt signal (black points) superimposed on the prediction without neutrino oscillation (blue dashed line) and the best fit with $\sin^2(2\theta_{13}) = 0.090$ (red line); background components after the fit are also shown (accidental in grey, ^{9}Li+^{8}He in green, fast neutron + stopping muons in magenta). *b*) Background-subtracted data on non-oscillating prediction as a function of the visible energy of the prompt signal (black points); overlaid is the best fit to the non-oscillation prediction (red curve) with reactor flux (green) and total systematic (orange) uncertainties

spectrum (shape) of each components is used, with data divided in energy bins, to characterize the oscillation as a function of E_ν/L and statistically separate the signal from the background. The major improvements of the *Rate + Shape* analysis of [6] are a wider energy range ($0.5-20$ MeV), a finer binning, which was possible thanks to the improved statistics, and a better energy reconstruction for IBD events. The off-off data is also included in the fit as an extra bin (pull term).

An independent analysis, or *Reactor Rate Modulation* (RRM), relies on the unique feature of Double Chooz experiment of having the direct background measurement given by the off-off period. This background model-independent method of θ_{13} compares the observed and expected IBD rate for different reactor power conditions in order to determine θ_{13} and total background at the same time. A RRM analysis applied to the lifetime of [7] was first reported in [10]. Two different approaches have been used: in the first one the background is treated as a total free parameter, while in the second approach the background is constrained usig the estimated value.

The results of the different analyses are resumed in Table 4.

Table 4. **Results of the different analysis in term of oscillation amplitude** $\sin^2(2\theta_{13})$ **and background rate**

Analysis	$\sin^2(2\theta_{13})$	Background rate, day^{-1}
Rate + Shape	$0.090^{+0.032}_{-0.029}$	1.38 ± 0.14
RRM (unconstrained background)	0.060 ± 0.039	$0.93^{+0.43}_{-0.36}$
RRM (constrained background)	$0.090^{+0.034}_{-0.035}$	$1.56^{+0.18}_{-0.16}$

8. ORTHO-POSITRONIUM OBSERVATION

Before undergoing annihilation, a large fraction of positrons form a metastable bound state with an electron of the medium called positronium (Ps). The formation probability of Ps depends on the material in which it forms. The Ps ground state has two possible configurations: para-positronium (p-Ps, B.R.: 25%), with total spin 0, and ortho-positronium (o-Ps, B.R.: 75%), with total spin 1. Both configurations are unstable, due to the possibility of e^+-e^- annihilation: in vacuum, p-Ps has a lifetime of 125 ps, while o-Ps lives three orders of magnitude longer (142 ns). However, matter effects result in a considerable shortening of the o-Ps mean life to a value depending on the material (a few ns).

While the p-Ps lifetime is short compared to the scintillation characteristic times, the formation of o-Ps introduces delay which separates the light pulse from the positron and the one from the annihilation gammas. This results in

a temporal time distortion of the global time profile, i.e., the pulse shape, of the event associated with the positron interaction. The distortion can be exploited to distinguish between electrons and positrons, and therefore reduces the cosmogenic background, in the framework of the well-established technique of the pulse shape discrimination.

The formation fraction and effective lifetime of o-Ps in Double Chooz scintillator was measured with a dedicated setup (see [11] for details), and the results are shown in Table 5. In the Double Chooz liquid scintillator — a mixture of dodecane, PXE, PPO and bis-MSB, doped with 1 g/l Gd [12] — the measured mean lifetime of o-Ps is (3.42 ± 0.03) ns. The pulse shape distortion induced by

Table 5. **Results on o-Ps analysis**

Setup	o-Ps fraction, %	o-Ps lifetime, ns
DC	$42 \pm 5(\text{stat.}) \pm 12(\text{syst.})$	$3.68 \pm 0.15(\text{stat.}) \pm 0.17(\text{syst.})$
NuToPs	47.6 ± 1.3	3.42 ± 0.03

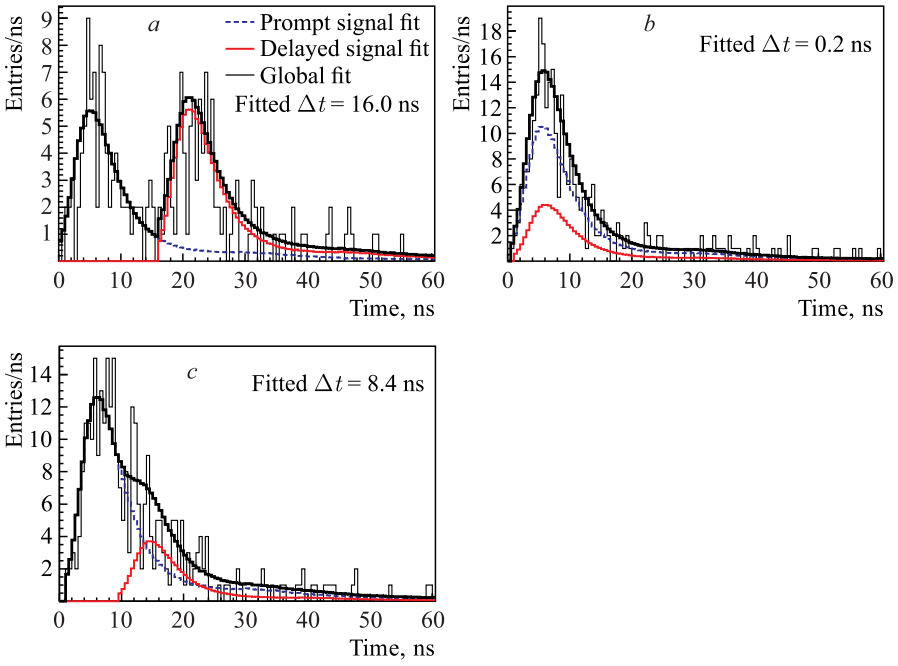

Fig. 4 (color online). Examples of o-Ps fit: the blue line represents the fit of the first signal, the red line the fit of the second one, and the black line is the total fit of the pulse shape

o-Ps with such a lifetime can hardly be used for a particle identification given the 2 ns sampling and the typical scintillating characteristic, which are times of the same order of magnitude. Nonetheless, we developed an algorithm that allowed us to observe the o-Ps on event-by-event basis, for the first time in a large liquid scintillator experiment.

A detailed description of the o-Ps tagging algorithm and the related results can be found in [13]. It is based on the identification of a double peak structure in the positron pulse shape: the first peak is given by the ionization and the second by the annihilation. The algorithm fits each signal with two reference

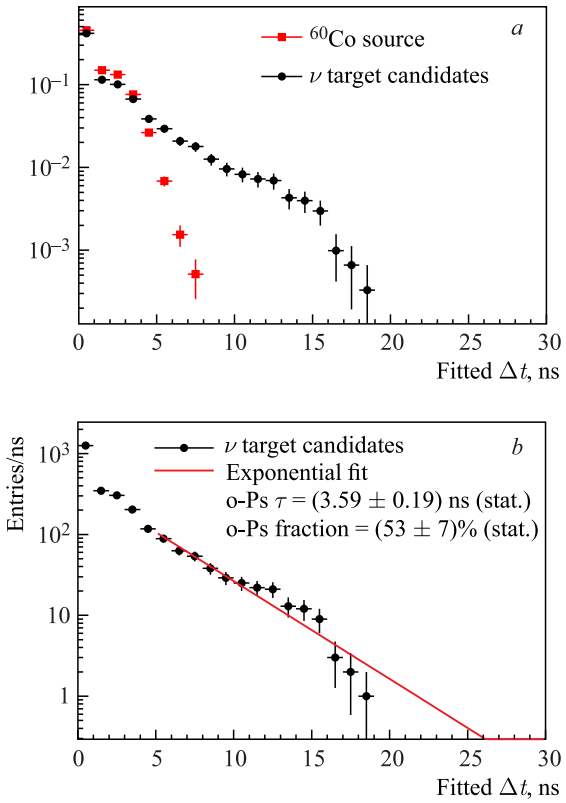

Fig. 5 (color online). *a*) The distribution of the Δt value determined by the fit for the cobalt sample (blue) is compared with the one for the neutrino candidates in the target (black), both normalized to one. *b*) The latter is fitted exponentially (red line) using ^{60}Co pulse shape as reference. From the fit the o-Ps lifetime and fraction are computed and the statistical error is given by the fit. The neutrino candidates (DC II publication [7]) have been selected in a visible energy range between 1.2 and 3 MeV

pulse shapes to extract the time delay between them Δt, which is left as a free parameter. The amplitude of the two pulses is constrained by energetic criteria: the second pulse energy must be 1.022 MeV, while the first one has to account for the rest of the energy. Few examples of fit are given in Fig. 4.

The fit was applied on events with energy between 1.2 and 3 MeV since at higher energy the first signal tail hides the second signal. The Δt spectrum obtained from the neutrino candidate sample [7] is compared to the one obtained with the ^{60}Co source, where no o-Ps is expected. As shown in Fig. 5, the distribution of the neutrino candidate sample shows a clear excess of events at larger Δt, enforcing the hypothesis of o-Ps. The o-Ps properties have been measured fitting the Δt distribution with an exponential. The distribution is fitted above 5 ns to exclude the region populated by the smearing observed in the ^{60}Co sample, as it can be seen again in Fig. 5. The fit result is sensitive to the choice of the reference pulse shape. The contribution to the systematic error accounting for this is evaluated as the semi-difference between the results obtained using two reference pulse shapes: a ^{60}Co source (high energies) and a ^{137}Cs source (low energies) ones. Other contributions to the systematics come from variations in the method of building the reference curves and from variations of the fit interval. The obtained results are in good agreement with the expectations (measured with the NuToPs dedicated setup [11]) and it can be seen in Table 5, confirming the first observation of o-Ps formation and paving the way for electron/positron separation in anti-neutrino experiments.

CONCLUSIONS

Double Chooz played a crucial role in the discovery of a non-zero value of the θ_{13} mixing angle and currently continues to contribute to its precision measurement. Double Chooz provided independent measurements on θ_{13} based on different analyses. It was the first experiment to report results with the H analysis [5] and, more recently, it published improved results with the Gd analysis [6]. In the latter, θ_{13} was obtained from a fit on the spectral shape of detected $\bar{\nu}_e$, for a measured value of $\sin^2(2\theta_{13}) = 0.090^{+0.032}_{-0.029}$. An independent analysis based on the reactor rate modulation, which does not assume any background parameterization but relies on its direct measurement profiting from both reactors off data, yielded consistent results: $\sin^2(2\theta_{13}) = 0.090^{+0.034}_{-0.035}$.

The Double Chooz near detector started to take data in the last Christmas (December 2014). The contribution of the near detector data will result in a reduction of the systematics — in particular on the neutrino flux estimation and detection — for a final precision on the $\sin^2(2\theta_{13})$ that is expected to be of about 10%.

Beyond the main experiment goal, other parallel analyses provided physics results: background studies were carried out [9], as well as studies on the Lorentz

violation [14], neutrino directionality and ortho-positronium detection on event-by-event basis. In particular, the o-Ps analysis and its implications on electron/positron separation could be a powerful additional handle for background rejection. This could be particularly appealing for experiments that look at sources like core-collapse supernovae, geo-neutrinos, or for nuclear reactor monitoring.

Acknowledgements. We acknowledge the financial support from the ANR NuToPs project (grant 2011-JS04-009-01) and from the UnivEarthS Labex program of Sorbonne Paris Cité (ANR-10-LABX-0023 and ANR-11-IDEX-0005-02).

REFERENCES

1. *Abe Y. et al. (Double-Chooz Collab.)* // Phys. Rev. Lett. 2012. V. 108. P. 131801.
2. *An F. P. et al. (Daya Bay Collab.)* // Ibid. P. 171803.
3. *Ahn J. K. et al. (RENO Collab.)* // Ibid. P. 191802.
4. *Abe K. et al. (T2K Collab.)* // Phys. Rev. D. 2013. V. 88. P. 032002.
5. *Abe Y. et al. (Double Chooz Collab.)* // Phys. Rev. B. 2013. V. 723. P. 66–70.
6. *Abe Y. et al. (Double Chooz Collab.)* // JHEP. 2014. V. 10. P. 1–44.
7. *Abe Y. et al. (Double Chooz Collab.)* // Phys. Rev. D. 2012. V. 86. P. 052008.
8. *Declais Y. et al. (Bugey Collab.)* // Phys. Rev. B. 1994. V. 338. P. 383.
9. *Abe Y. et al. (Double Chooz Collab.)* // Phys. Rev. D. 2013. V. 87. P. 011102.
10. *Abe Y. et al. (Double Chooz Collab.)* // Phys. Lett. B. 2014. V. 735. P. 51–56.
11. *Consolati G. et al.* // Phys. Rev. C. 2013. V. 88. P. 065502.
12. *Aberle C. et al.* // JINST. 2012. V. 7. P. P06008.
13. *Abe Y. et al. (Double Chooz Collab.)* // JHEP. 2014. V. 10. P. 1–17.
14. *Abe Y. et al. (Double Chooz Collab.)* // Phys. Rev. D. 2012. V. 86. P. 112009.